

A NOVEL METHOD FOR SHOEPRINTS RECOGNITION AND CLASSIFICATION

MIN-QUAN JING, WEI-JONG HO, LING-HWEI CHEN

Department of Computer Science and Engineering, National Chiao Tung University, Hsinchu, Taiwan 300, ROC
E-MAIL: mqjing@msn.com, reyalp@debut.cis.nctu.edu.tw, lhchen@cc.nctu.edu.tw

Abstract:

In this paper, we present a method for automatically classifying/recognizing the shoeprint images based on the outsole pattern. Shoeprints are distinctive patterns often found at crime scenes that can provide valuable forensic evidence. Directionality is the most obvious feature in these shoeprints. For extracting features corresponding to the directionality, co-occurrence matrices, Fourier transform, and a directional matrix are applied to the shoeprint image. With the stage of principal component transform, the method is invariant to rotation and translation variance. Experimental results demonstrate the performance of the method.

Keywords:

Forensic science; Shoeprint; Fourier transforms; Co-occurrence matrix; Principal component transform

1. Introduction

Crime scene is the location where the crime has been committed or found. Many valuable clues left behind by criminals may be collected at crime scene so that crime scene investigation takes a crucial role of case solving in the modern time. At present, fingerprints, bloods, hairs, and shoeprints are all common evidences taken by scientists or investigators at crime scenes. However, while both fingerprints and DNA have been studied frequently and some effective methods have been developed for recognition, researches on shoeprints recognition are rarely noted. Therefore, developing an effective method for automatically classifying/recognizing the shoeprint images will greatly help the crime scene investigators to identify shoeprint impressions.

Shoeprints - the marks made by the outsole surface of shoes - are the most common clues left at crime scenes. A report from Girod [1] revealed that approximately 30% of all burglaries provide usable shoeprints that may be recovered from crime scene, while another study of several jurisdictions in Switzerland [2] found that 35% of crime scenes had shoeprints usable in forensic science. These statistics all manifest the value of shoeprint as forensic

evidence. From other view, shoeprints, unlike fingerprints or other type of physical evidence, generally cannot uniquely identify an individual. Nevertheless, due to the wide variety of shoes available on the market, with most having distinctive outsole patterns, this implies that any specific model of shoe will be owned by a very small fraction of the general population [3]. Hence, with a collected model of a shoeprint, the searching range of suspects could be significantly reduced.

Ordinary method for matching shoeprint images is carried out manually by searching through paper catalogues or computer database. The searching process is laborious and tedious, and worst of all, time-consuming. Some semi-automatic methods have been developed to improve the efficiency [4-5]. These methods use a palette of basic elements composed of visible shapes to construct a model of a shoeprint pattern. But while modern shoeprints are having increasingly intricate sole patterns, it is hard to characterize these patterns with limited elements. Not many of the automatic approaches have been reported widely. Bouridane et al. [6] proposed an automatic shoeprint recognition method based on fractal decomposition. Fractals are used to represent the shoeprints and the final match is given based on the Mean Square Noise Error method. The disadvantage of the method is that it could only tolerate small translations and rotations. Chazal et al. [7] utilize Fourier transform and calculate the power spectral density (PSD) to sort the shoeprint database with respect to the query image. The orientation variance is conquered by having multiple PSD images with various representative angles; hence the matching procedure would be exhausting. In this thesis, we propose an automatic shoeprint recognition method, which utilizes principal component transform to conquer the orientation variances. And with the adoption of various feature vectors, the proposed method is concise and effective.

The rest of the paper is structured as follows. Section 1 describes the shoeprint images used in the study. The proposed recognition method is discussed in Section 2. The

proposed method has been evaluated by experiments as reported in Section 3. The final section closes the paper with conclusion and future research.

2. The proposed method

The flow diagram of the proposed method is shown in Fig. 1. The whole process consists of three major phases: preprocessing, feature extraction, and pattern matching. In the preprocessing phase, a shoeprint image is processed with some techniques to eliminate distortions for further manipulation. In the feature extraction phase, the preprocessed image is processed using different directionality measures to extract features for pattern matching. In the pattern matching phase, based on the extracted features, a similarity measure is provided. On the basis of the similarity measure, the shoeprint image in the database that is most similar to the input image is determined.

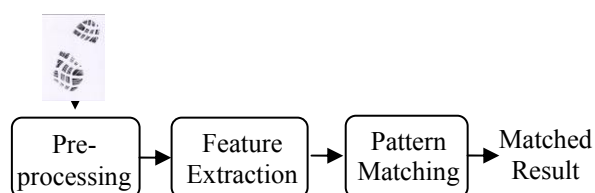


Figure. 1. Flow diagram of the proposed method

2.1. Preprocessing

Owing to the instability during imprint and scanning process, shoeprint images captured from imprint and digitization would suffer many distortions. These distortions include rotation, translation, imprint noise and other disturbances. The aim of this stage is to reduce these distortions and produce a standard format for feature extraction.

2.1.1. Gray-scale transformation

Original shoeprint images are of 16777216 (2^{24}) color level. To transform color images into gray-scale ones, we apply the following equations:

Let

$R(i, j)$ denote the red value at pixel (i, j)

$G(i, j)$ denote the green value at pixel (i, j)

$B(i, j)$ denote the blue value at pixel (i, j)

Then the transformation [8] is

$$gray(i, j) = 0.257 * R(i, j) + 0.504 * G(i, j) + 0.098 * B(i, j) + 16. \quad (1)$$

2.1.2. Noise removal, Smooth, and Edge detection

Noises of an image could cause disturbing values in the print. To eliminate noises occurring from imprint and scanning process, images are divided into blocks, each of size $16*16$. For each block B , we calculate its mean and variance. If the variance of the block is lower than a specified threshold, the entire block is set to white color value (that is, the gray level of each pixel in the block is 255). Otherwise, keep the original contents.

After block-based noise removing, we apply the $5*5$ Gaussian low-pass filter [9] to each pixel of the shoeprint image for further elimination of tiny noises. In order to preserving the structure properties in an image, the Sobel operator is used to extract the edges for the shoeprints. Finally, a threshold based bi-level thresholding method designed to extract high spectral pixels from the shoeprint image. After the bi-level thresholding, The entire image is of only two values then, pure black and pure white.

2.1.3. Principal component transform

The orientations of the shoeprint images are of multiple variations. These rotations bring about a problem for feature extraction due to inconsistency of shoeprint images. To solve this problem, we make use of principal components for variable orientations. Aligning the image with its principal eigenvectors provides a reliable mean for removing the effects of rotation. Fig. 2(a) is the original shoeprint image. Fig. 2(b) shows the shoeprint image with its corresponding eigenvectors drawn with dashed lines. Fig. 2(c) is the one transformed with respect to the eigenvectors of the largest eigenvalue.

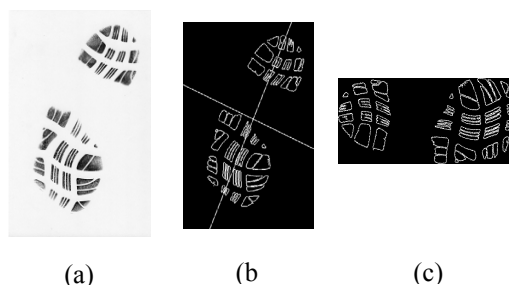


Figure2. An example of principal component transform (a) Original shoeprint image. (b) The shoeprint image with its corresponding eigenvectors. (c) The transformed shoeprint image.

2.2. Feature extraction

The most obvious pattern in shoeprints is directionality. The shoeprint images shown in Fig. 3 present the patterns of vertical lines, circular shapes, and various geometries. These drafts all represent a unique model of its own pattern. Therefore, a feature extraction method based on directionality is designed. To estimate the energy of each direction in the whole image, three different approaches are provided. The first one uses co-occurrence matrices to calculate the relation between pixels. The second uses a region based direction mask to compute the local ridge orientation for the entire image. The third takes global directionality, enhanced Fourier transform extends from normal Fourier transform is employed. Taking only global characteristics into consideration, however, might lose some local information. For the sake of this flaw, enhanced Fourier transform is also applied to local areas of the shoeprint to extract local information.

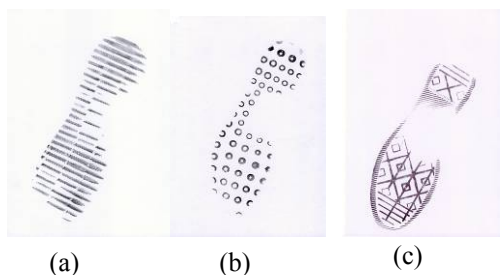


Figure3. An example of shoeprint patterns (a) Vertical lines. (b) Circular shapes

2.2.1. Co-occurrence matrices

Co-occurrence matrix, which was first introduced by Haralick in 1979 [10], is defined over an image to be the distribution value of co-occurring values at a given offset. Here we will introduce the definition of co-occurrence matrices and its characteristics for an image. Let T be an image of 2 color level (pure black and pure white), $L(p, q)$ be the intensity value of pixel (p, q) in image T and $v = (\Delta x, \Delta y)$ be an offset vector. The co-occurrence matrix $C_v(i, j)$ is the 2×2 matrix defined as follows:

$$C_v(i, j) = \sum_{p=1}^n \sum_{q=1}^m \begin{cases} 1, & \text{if } L(p, q) = i \text{ and } L(p + \Delta x, q + \Delta y) = j \\ 0, & \text{otherwise} \end{cases} \quad (2)$$

Then a point (i, j) in C counts the number of pixel

pairs in T that have respectively intensity i and j with displacement offset v . It can be seen that co-occurrence matrix collects the second-order statistics of image T with the characteristics that the main diagonal of the matrix with offset v is as closer to the histogram of the image as v is related to the corresponding direction [11]. Based on this observation, we propose a measure as follows: Let $H(i)$ be the histogram of the image, $i = 0, 255$. The discrepancy of co-occurrence matrix C , $D(v)$ is defined by

$$D(v) = \frac{1}{2}(H(0) - C_v(0,0) + H(255) - C_v(255,255)) \quad (3)$$

In order to obtain the properties of directionality, the discrepancy value must be computed for a set of offset vectors V . Let $CM(v) = 1 - D'(v)$ be the relevant value to the direction v , where $D'(v)$ denotes the normalized value in $[0, 1]$ of $D(v)$. Then $CM(v)$, $v \in \{(i, j) | i = -4, -3, 3, 4 \text{ and } j = -4, -3, 3, 4\}$ is selected as a feature vector for pattern matching. Note that the normalization for $D(v)$ is defined by

$$D'(v) = \frac{D(v) - \min V}{\max V - \min V} \quad (4)$$

where $\min V$ and $\max V$ denote the minimum value and the maximum value of all $D(v)$ with $v \in V$ respectively.

Fig. 4(b) shows the $CM(v)$ value of the Fig. 4(a). Each square with coordinate (i, j) relative to the image center represents the offset (i, j) . Pure black means the strongest response, while pure white means the slightest response. Solidus regions are unconsidered offset values. Note that offsets with $|i| < 2$ and $|j| < 2$ are not considered because it will cause noisy information.



Figure4. Result of the co-occurrence matrix. (a) The edge points of an input shoeprint image. (b) An gray-level representation of CM

2.2.2. Directional mask

Co-occurrence matrix gives the behavior between pairs of pixels according to the offsets. However, due to the noises in shoeprints, the relevance measure of

co-occurrence matrix might be incorrect. To obtain relevance of directionality from another view, directional masks are proposed. 12 masks, each of size 7*7, refer to predefined directions 0°, 15°, 30°, 45°, 60°, 75°, 90°, 105°, 120°, 135°, 150°, 165°, as shown in Fig. 5 are used.

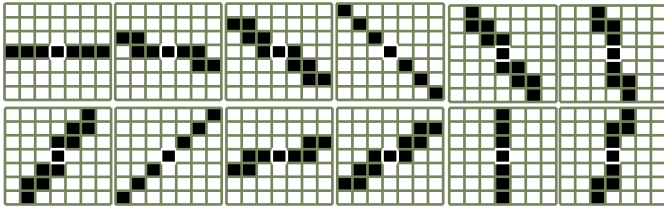


Figure 5. Twelve directional masks of 0°, 15°, 30°, 45°, 60°, 75°, 90°, 105°, 120°, 135°, 150°, 165°.

The steps for ridge direction retrieval are describing as follows. At first, for an input preprocessed shoeprint image of size $n \times m$, sliding the k th mask through the image, compute the convolution for each pixel as follows:

$$O_k(i, j) = \sum_{p=1}^7 \sum_{q=1}^7 L(i+p-4, j+q-4)M_k(p, q) \quad (5)$$

where $M_k(p, q)$ denotes the value of mask M_k at pixel (p, q) . And then the energy for each direction is

$$D(k) = \sum_{p=1}^n \sum_{q=1}^m \begin{cases} 1, & \text{if } O_k(p, q) \geq \frac{2}{3}(\text{number of 1s in } M_k) \\ 0, & \text{otherwise} \end{cases} \quad (6)$$

, for $k=1, \dots, 12$

$DM(k), k=1, \dots, 12$ is selected as a feature vector for similarity measurement, where $DM(k)$ denotes the normalized value in $[0, 1]$ of $D(k)$.

2.2.3. Global Fourier Transform

The Fourier Transform is widely employed for processing image to analyze the frequencies contained in an image. In this section, we first make use of the Fourier Transform to evaluate the strength of directionality over the image. Then, the masking operation is performed to remove the high-frequency and low-frequency noises. After applying Fourier transform on the target image, we perform the Fourier transform on the Fourier spectrum again to get the enhanced Fourier Spectrum. The enhanced Fourier spectrum is more prominent than the original spectrum. It reinforces the peaks with the same periods and contributes to the same frequency while for those which are not periodic ones, they do not contribute to the same frequency [12].

This phenomenon relatively enhances those peaks and eliminates the non-periodic noises in an image. Fig. 6(a) shows the Fourier spectrum of the target image in Fig. 4(a). Fig. 6(b) is the Fourier spectrum image obtained by applying Fourier transform on Fig. 6(a).

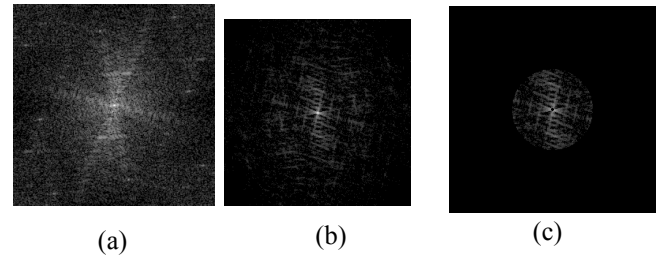


Figure 6. An example of the enhanced Fourier spectrum and the masking operation. (a) The Fourier spectrum of Fig. 4(a). (b) The enhanced Fourier spectrum of (a). (c) The spectrum with low-frequency and high-frequency masks apply on (b)

To remove slowly varying components such the needless components, a mask for removing low-frequency elements is applied. High-frequency components which occur owing to outsole scuffs and nicks of the shoe may result in outstanding values over the underlying shoeprint patten [7]. Similarly, a mask for removing the high-frequency components is applied. Only frequencies that have Euclidean distance less than a predetermined threshold from the zero spatial-frequency point are preserved as candidate features. Fig. 6(c) shows the spectrum with both high-frequency and low-frequency masks applied on Fig. 6(b).

2.2.4. Local Fourier Transform

The local Fourier Transform is used to compensate the problem of lose details in local area. The processed shoeprint image is divided into 15 equal regions as shown in Fig. 7(a). Following that, Fourier transform is performed on each region twice to get the enhanced Fourier spectrum of the area.

Low-frequency mask and High-frequency mask are also applied on each region k to get the masked Fourier spectrum F'_k . The remaining values, which are denoted by $LF = \{F'_k(i, j) | k=1, \dots, 15 \quad i=1, \dots, n/5 \quad j=1, \dots, m/3 \quad (i, j) \text{ is neither in high-frequency nor in low-frequency areas}\}$, are selected as a feature vector.

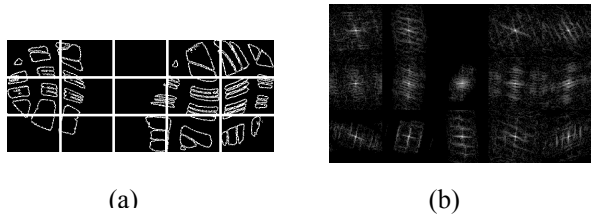


Figure 7. An example of local Fourier transform. (a) A representation of dividing an image into 15 equal regions. (b) The result of applying local Fourier transform of Fig. 7(a)

2.3. Pattern matching

Feature vectors extracted from the operations described above, including *CM*, *DM*, *GF*, and *LF*, are taken for pattern matching at this stage. In order to obtain the most likely shoeprint image that compares to the reference image, we use sum-of-absolute-difference (SAD) as the similarity measure. Let images *T* and *T'* be the database image and reference image respectively, the similarity between the selected feature vector of the image pair is calculated by

$$S(F) = \frac{1}{K} \sum_{i=1}^K |F_i'' - F_i'| \tag{7}$$

where F_i denotes the i^{th} element of a feature vector F , and $F \in \{CM, DM, GF, LF\}$. K denotes for the number of elements in the feature vector. F is a feature vector belongs to T . F' is a feature vector belongs to T' .

Prints of databases are then sorted according to the similarity measure with the most similar image shown at the front of the results. Scores are given to the sorted categories of database from 1 to 90.

2.4. K-means algorithm for database creation

We use the K-means algorithm to select representative images as the database category for each of the print sets. Feature vectors *CM*, *DM*, *GF* and *LF* are taken as attributes $f = \{CM, DM, GF, LF\}$, and used in the K-means algorithm to form three groups. From each group, the image with the closest distance to the centroid of the group is taken as the representative image. And then the selected three images are taken as database images. Seven of others are taken as query images.

3. Experimental result

Here, 300 shoeprint images collected from 30 distinct shoes are used to test our algorithm. 90 out of 300 prints are taken as the database images according to the K-means process described above. The remaining shoeprint images become the query images. Fig. 8 shows some distinct shoeprints. Every print in the database is examined in turn for comparison with the input shoeprint. The similarity measures calculated based on each feature vector are then used to sort the shoeprint images in the database from the most similar print to the least similar one.



Figure 8. Shots of 30 distinct shoeprints

The method is designed to find similar shoeprints and sort the corresponding categories of database in response to a reference image. With higher performance, the result is expected to present fewer nonmatching shoeprint categories before a matching category. Table 1 shows the query results. With respect to the query shoeprint, each row shows the top 5 query results according to different feature vectors. In the first row, taking the feature vector of co-occurrence matrix, the correct matching is delivered in the 3rd, the 4th, and the 5th position. While taking all features into consideration, the correct matching is delivered in the 1st, the 2nd, and the 4th position. Each feature vector is conducted independently first, and then combined together for further assessment. The best performance is the one with the combination of all proposed features vectors.

Table1. The query results

		Query Results				
		1 st	2 nd	3 rd	4 th	5 th
Query shoeprint	Co-occurrence					
	Direction					
	Global Fourier					



4. Conclusion

The study proposed a novel method for automatically recognizing the shoeprint image using the properties of directionality. Experiments showed the accuracy and efficiency of the proposed method. It can accelerate human observer identifying the shoeprint pattern with respect to the reference image. Improvements may be achieved by employing new de-noise methods in preprocessing and delicately designed the database images from acquired shoeprints.

Acknowledgements

This work is supported in part by National Science Council (NSC 97-2221-E-009-137-).

References

- [1] A. Girod, "Computer Classification of the Shoeprint of Burglar Soles," *Forensic Science Int'l*, vol. 82, pp. 59-65, 1996.
- [2] A. Girod, "Shoeprints - Coherent Exploitation and Management," European Meeting for Shoeprint/Toolmark Examiners, The Netherlands,

- 1997.
- [3] W.J. Bodziak, "Footwear Impression Evidence Detection," *Recovery and Examination*, 2nd ed. CRC Press, 2000.
- [4] N. Sawyer, "'SHOE-FIT' A Computerized Shoe Print Database," *Proc. European Convention on Security and Detection*, pp. 86-89, May 1995.
- [5] W. Ashley, "What Shoe Was That? The Use of Computerized Image Database to Assist in Identification," *Forensic Science Int'l*, vol. 82, pp. 67-79, 1996.
- [6] A. Bouridance, A. Alexander, M. Nibouche, and D. Crookes, "Application of Fractals to the Detection and Classification of Shoeprints," *Proc. 2000 Int'l Conf. Image Processing*, vol. 1, pp. 474-477, 2000.
- [7] P. de Chazal, J. Flynn, and R. B. Reilly, "Automated Processing of Shoeprint Images Based on the Fourier Transform for Use in Forensic Science," *IEEE Trans. Pattern Analysis and Machine Intelligence*, vol. 27, no. 3, pp. 341-350, March 2005.
- [8] K. Jack, "Video Demystified," 5th ed. Elsevier, 2007.
- [9] R. Fisher, S. Perkins, A. Walker, and E. Wolfart, "Image Processing Learning Resources," <http://homepages.inf.ed.ac.uk/rbf/HIPR2/gsmooth.htm>
- [10] R. M. Haralick, "Statistical and Structural Approach to Texture," *Proc. IEEE*, vol. 67, no. 5, pp. 786-804, 1979.
- [11] A. K. Julesz, "Dialogues on Perception," MIT Press, Cambridge MA, 1995.
- [12] K. L. Lee, L. H. Chen, "A New Method for Coarse Classification of Textures and Class Weight Estimation for Texture Retrieval," *Pattern Recognition and Image Analysis*, vol. 12, no. 4, pp. 400-410, 2002.